EXPERIMENTAL PROCEDURES

Plasmid Constructs. Site-directed mutagenesis was performed using the QuikChange method (Stratagene/Agilent) resulting in specific mutations in the K18 311/328 double cysteine construct (K18 311/328 cloned into pET28b).[1] The following mutations were introduced: ΔK280 (deletion at position 280), P301S, I308M, P312I, D314I, S320F, G323I, G326I, and Q336R. The correctness of all constructs was confirmed by DNA sequencing.

Protein Expression and Purification. Expression and purification were performed as previously described.[2] In short, overnight cultures of transformed *Escherichia coli* bacteria (BL21(DE3)) were diluted 1:100 with LB medium (Miller, BD) and incubated at 37 °C until the optical density reached ~0.8 at 600 nm. Protein expression was induced by addition of 1 mM isopropyl-β-D-thiogalactopyranoside (IPTG, Gold Biotechnology) and allowed to continue for at least 3.5 hours at 37 °C. The bacteria were then pelleted at 3,000 X g, resuspended in 20 mM piperazine-*N*,*N*'-bis(2-ethanesulfonic acid) (PIPES, J.T. Baker) pH 6.5, 500 mM NaCl, 1 mM ethylenediaminetetraacetic acid (EDTA, J.T. Baker), and 50 mM β-mercaptoethanol (MP Biomedicals) buffer, and stored at –80 °C. Protein extraction began by incubating the bacteria for 20 minutes at 80 °C followed by sonication on ice. The samples were centrifuged at 15,000 X g for 30 min to separate soluble protein from cellular debris. The supernatant was added to 55% w/v ammonium sulfate (MP) and incubated at room temperature for 1 hr. Precipitated tau protein was collected by centrifugation at 15,000 X g for 10 min. The pellet was resuspended in H_2O to which 2 mM dithiothreitol (DTT, Gold Biotechnology) was added to maintain a reducing environment. After filtration the protein sample was loaded onto a Mono S (GE Healthcare) cation exchange column, to which a linear NaCl gradient was applied (50 – 1000 mM NaCl, 20 mM PIPES pH 6.5, 2 mM DTT). Fractions were assessed by SDS -PAGE and pooled appropriately. To achieve further purification, samples were loaded onto a Superdex 200 (GE Healthcare) gel filtration column and eluted with a 20 mM Tris (Sigma), 100 mM NaCl, 1 mM EDTA, and 2 mM DTT buffer at pH 7.4. Fractions containing pure tau were combined and precipitated overnight at 4 °C using a 3-fold volumetric excess of acetone to which 5 mM DTT was added. Pellets were collected at 15,000 X g and stored in 2 mM DTT/acetone at –80 °C.

Protein Labeling. Purified protein pellets were dissolved in 200 μL 8 M guanidine hydrochloride (Thermo). Double-cysteine mutants were labeled by addition of a 10-fold molar excess of the spin label [1-oxyl-2,2,5,5-tetramethyl-Δ3-pyrroline-3-methyl]methanethiosulfonate (MTSL, Toronto Research Chemicals) and incubated at 25 °C for 1 hr. The mutants, along with K18 WT (two natural cysteines replaced by serines), were passed over PD-10 columns (GE Healthcare) to remove excess label and guanidine HCl. Protein eluted with 10 mM 4-(2-hydroxyethyl)-1-piperazineethanesulfonic acid (HEPES, J.T. Baker), 100 mM NaCl, and 1 mM NaN_3 buffer at pH 7.4. Concentrations were determined using the bicinchoninic acid (BCA) assay (Pierce). Labeling efficiency was similar for all K18 311/328 mutants, as shown by room temperature continuous wave EPR on a Bruker EMX Plus spectrometer fitted with an ER 4119HS resonator. CW spectra are shown in Figure S5 a; the integrated signal intensity was 3.2 ± 0.1 e11 for all mutant monomers diluted to 10 μM (concentration confirmed on 15 % SDS - PAGE, Figure S5 b).

Fibril Assembly. Tau fibrils were prepared by combining 2% labeled K18 311/328 with 98% K18 WT with a total protein concentration of 50 μM, along with 12.5 μM heparin cofactor (Celsus) and 10% K18 WT seeds (preparation described below). Fibrils were allowed to grow overnight during 37 °C incubation. Following centrifugation (100,000 X g) and washing, pellets were resuspended in 10 - 30 μL buffer (10 mM HEPES, 100 NaCl, 1 mM NaN_3 at pH 7.4) and transferred into 1.6 mm outer diameter quartz Q-band EPR tubes. Excess buffer was removed after centrifugation (1000 X g) of the samples. CW EPR was performed at room temperature to probe for short distance spin interactions that can interfere with analysis of DEER data (Figure S7). Spectra were taken at an incident microwave power of 12 mW. After measurement, samples were immediately frozen in liquid N_2 and stored for no longer than one month at –80 °C to await DEER analysis.

Preparation of Seeds. K18 WT fibrils were formed by stirring a mixture of 25 μM K18 WT monomer and 12.5 μM heparin cofactor in buffer (10 mM HEPES, 100 NaCl, 1 mM NaN_3 at pH 7.4) for three days at room temperature. These fibrils were sonicated (Fisher Scientific tip sonicator, D100 series) for 20 s on ice, breaking them into small fragments used as seeds. 10%

of these seeds were added to 25 μM K18 WT monomer and 50 μM heparin in buffer, and fibrils grew for 1 h at 37 °C. The new fibrils were sonicated in the same manner to create new seeds. This series of sonication and incubation was performed 5 times, the final time corresponding to preparation of the DEER samples in which K18 WT was mixed with labeled K18 311/328. The formation of seeds through the multistep procedure has been described previously.[1] These seeds, which provide the templates onto which the tau monomers grow, contain a heterogeneous mixture of fibril conformations from which the monomer can select. These populations of conformers may be influenced by initial seed growth conditions, leading to slight variations in peak height of DEER distance distributions. We therefore used seeds formed from the same preparation outlined here for all samples analyzed by DEER. Slight variations seen in distance distributions do not impact fibril growth kinetics, so different seed batches have been used for some of these experiments.

Collection of DEER Data. DEER measurements were performed at Q-band (34 GHz) on a Bruker E580 pulse spectrometer. The Bruker ER 5107D2 dielectric resonator was fully overcoupled ($Q \sim 500$) to reduce resonator ringdown. Measurements were taken at 80 K using an Oxford CF 935 cryostat. Dipolar evolution curves were collected via 4-pulse DEER according to the scheme in Figure S13. The $^{\pi}/_{2}$ observer pulse at ν_1 was adjusted for each experiment to give the maximum echo height and ranged from 36 – 42 ns. The π pump pulse at ν_2 was 40 ns. τ_1 and τ_2 were held constant for each experiment at 200 and 2500 ns, respectively. The pump pulse started at t = 100 ns and was stepped in 8 ns increments. A field-swept echo-detected spectrum was recorded before each DEER experiment to find the field position of the echo maximum. The pump frequency (ν_2) was set to the center of the resonator dip, corresponding to the center of the field-swept spectrum. The observer frequency (ν_1) was adjusted 37 MHz below the pump frequency, corresponding to the position of highest intensity in the field-swept spectrum. Any two pulses form an echo, so 8-step phase cycling was used to remove unwanted echoes. Spectra were averaged between 48 – 120 hrs, depending on signal strength. The shot repetition time (SRT) was set to 1.2 times the T_1 measured by 3-pulse inversion recovery. The T_1 for nitroxides similar to MTSL at 80 K are determined primarily by the local environment.[3] In the compact fibril structures, little variation in environment is

expected at the positions of the two labels. The T_1 value measured by inversion recovery for all mutants, including 311/328 in triplicate is 490 +/- 50 μs. The small variation in T_1 is consistent with the expectation of similar environments. The electron-electron interspin distances in these samples are too long to have significant impact on T_1[4] so changes in conformation that impact interspin distance do not change T_1. The length of the time trace (τ_2) was limited by the relatively short spin echo phase memory dephasing times for the nitroxides in the fibrils, T_m = 1.46 +/- 0.07 μs. This window restricts distance information to less than about 5.2 nm, which is the reason for the extent of the calculated profiles in the figures.

Analysis of DEER Data. Raw DEER data were analyzed with "DEERAnalysis2011"[5] using Tikhonov regularization. The background arises primarily from electron-electron spin-spin interaction of each of the nitroxides with nitroxides other than the partner on the same monomer unit. These interactions were decreased by diluting the spin-labeled monomers with 98% unlabeled K18 WT, but are still significant. The DEER data for fibrils grown from singly labeled monomers (either 311 or 328) fit well to a homogeneous 3D model, so the same model was used for analysis of data. The calculation of the background correction consistently excluded the early portions of the time trace as shown in the Figure S1 b, S8 b, and S9 b. There is little variation in the distance distributions obtained by altering the start of background subtraction. Figure S2 shows two extremes in background fit. Background subtraction parameters were chosen that gave the best fit to a well-resolved Pake doublet (Figure S1 c, S8 c, S9 c), and were consistent for all samples. The regularization parameter (α) of 100 was selected as the intersection point on the L-curves, which are shown in Figure S1 a, S8 a, and S9 a, giving the best compromise between peak resolution and smoothness. The L-curves are very similar for all samples, and the choice of α = 100 was kept constant for accurate comparison between samples.

The distance distributions computed using the above parameters gave an ensemble of peaks, as was shown previously for K18 311/328.[1] To examine variation in the distance distributions between mutations, Tikhonov regularization was used because it does not constrain the resulting distances to a set number of Gaussians, single, double, or triple. Two tests were performed to check the reliability of the results obtained with DEERAnalysis. 1) An additional program,

GLADD (Global Analysis of DEER Data),[6] was used for comparison of the main features. GLADD is a program that determines the most probable background subtraction and distance distribution simultaneously. The program uses no *a priori* background correction and can fit data to single, double, or triple Gaussian models. While the double Gaussian distance distribution obtained using GLADD shows features that are similar to the Tikhonov fit in DEERAnalysis, the sharpness of the peak around 4.8 nm was a concern. Data were collected for K18 311/328 at 60 K with τ_2 of 3500 ns, an increased window size, and GLADD analysis showed broadening of the sharp peak (Figure S14). These analyses indicate that the peak at 4.8 nm is needed to fit the data. However, the limitation to only two Gaussians does not provide a way to model the multiple components at shorter distances that are obtained by Tikhonov regularization. 2) In DEERAnalysis the peak at 4.8 nm was removed using peak suppression. The resulting simulation of the raw data was in very poor agreement with the experimental data, which showed that the distance of 4.8 nm is required to fit the experimental data (Figure S15). The validation feature of DEERAnalysis allows variation in the background subtraction parameters; little change to the distance distribution was seen when altering the starting point of background subtraction (Figure S2), suggesting that appropriate parameters were used for this class of samples.

Thioflavin Assay. Kinetics of K18 seeded reactions were assessed by thioflavin T (ThT) fluorescence at 37 °C. ThT (Sigma T3516) and K18 monomers were present at 5 μM and 10 μM, respectively, in 100 mM NaCl, 10 mM HEPES, pH 7.4 buffer. Monomers were pre-incubated at 37 °C for 5 min and aggregation initiated by the addition of 4% K18 WT seeds and 20 μM heparin. Fibril assembly was measured in a Fluorolog 3 fluorometer (Horriba Jobin) with excitation wavelength set at 440 nm and emission wavelength set at 480 nm (slit widths = 5 nm). Spin-labeled K18 311/328 and its ΔK280 mutant did not affect aggregation kinetics (Figure S3).

Recruitment of K19 Monomers with ΔK280 K18 Seeds. Fibril seeds were formed by combining 25 μM tau monomer with 50 μM heparin in buffer (100 mM NaCl, 10 mM HEPES, pH 7.4), and incubating at 25 °C under stirring conditions for 3 days. Fibrils were sheered by sonicating 500 μL of sample for 20 seconds with a microtip sonicator. For sedimentation

experiments 10% molar K18 WT or ΔK280 K18 seeds were added to 10 μM K19 WT monomer in buffer with 20 μM heparin, and incubated for 3 hours at 37 °C. Samples were centrifuged at 100,000 X g for 30 minutes at 10 °C. Pellets were resuspended with 40 μL 1X SDS PAGE sample buffer and aggregated tau was assessed by SDS PAGE.

Acrylodan Fluorescence Assay. Aggregation of tau monomer was determined using an intrinsic acrylodan fluorescence assay previously described.[7] Briefly, K19 was labeled at position 310 (tyrosine substituted with cysteine) with a 10-fold molar excess of acrylodan. After removal of excess dye, 2% labeled K19 was mixed with 98% K19 WT (cysteine replaced with serine) at a total protein concentration of 10 μM. Aggregation reactions were initiated by addition of 10% seeds (K19 WT, K18 WT or ΔK280 fibrils, sonicated) and 20 μM heparin in 100 mM NaCl, 10 mM HEPES, pH 7.4 buffer. Samples were measured with excitation wavelengths set at 360 nm and emission wavelengths scanned from 400-600 nm (5 nm slit widths). Temperatures were maintained at 37 °C with a solid state Pelletier element. Spin labeled K18 311/328 and its ΔK280 variant do not affect the overall growth characteristics of K18 WT (Figure S3).

Negative Stain Electron Transmission Microscopy. Tau fibril samples were prepared and analyzed as previously reported[1] using 20 μM protein concentrations. Images were taken with a Philips/FEI Tecnai-12 electron transmission microscope at 80 keV and equipped with a Gatan CCD camera. All samples contained fibrils (Figure S6).

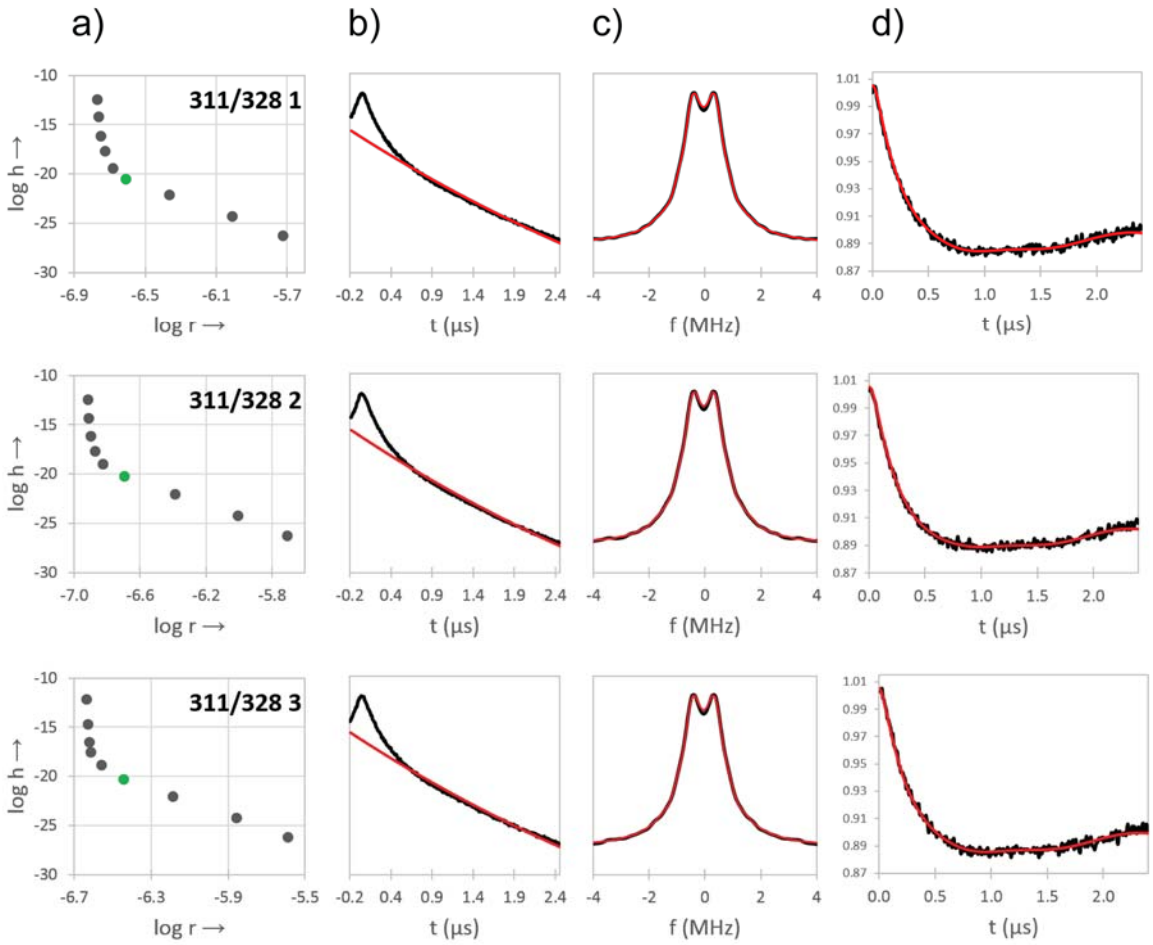

Figure S1. DEER data analysis of K18 fibrils labeled at positions 311/328. a) L-curves. b) Background fits. b) Pake patterns. d) Background subtracted DEER data. Fit lines are in red, and $\alpha = 100$ is in green on the L-curve. The different rows represent independent experiments.

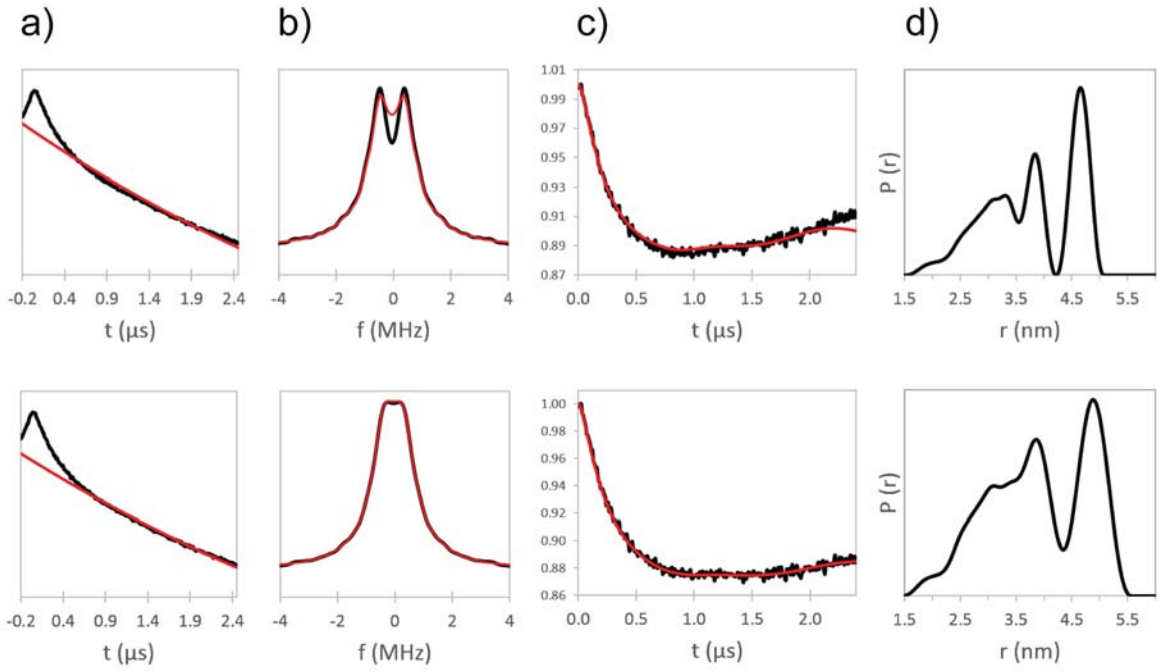

Figure S2. Effect of Background fits on distance distribution. a) Background fits. b) Pake patterns. c) Background subtracted DEER data. d) Distance distributions. Fit lines are in red. The top and bottom rows represent two extremes in background fit. If background subtraction is positioned too early in the trace (top row, a), the Pake doublet is well separated, but the fit is poor (top row, b). If positioned too late (bottom row, a), the Pake splitting is diminished (bottom row, b), although the fit is improved. Throughout our analysis, background subtraction parameters were chosen that gave the best fit to a well-resolved Pake doublet, and were consistent for all samples. Importantly, the two extremes in background fit do not alter the peak positions, only the peak heights.

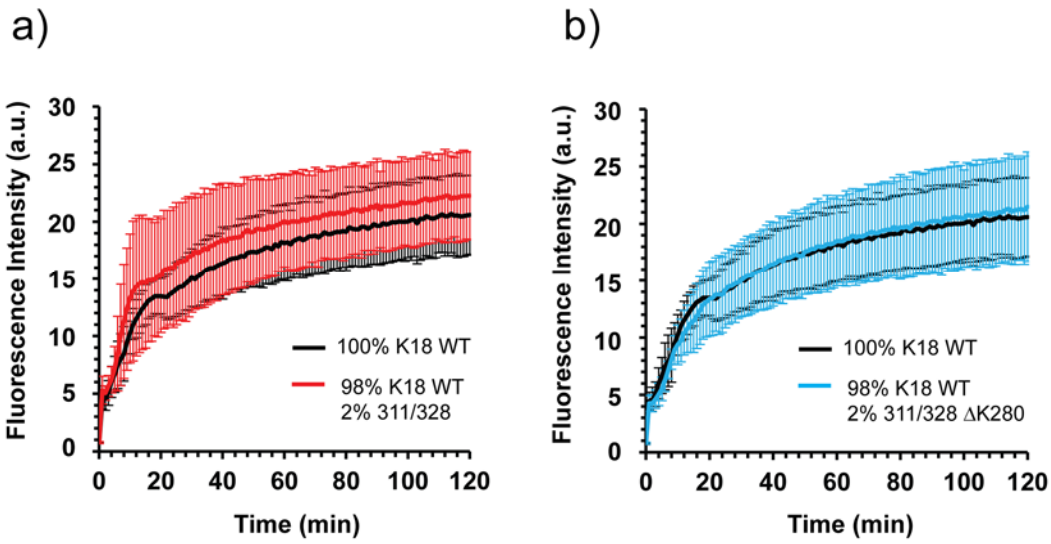

Figure S3. Seeded growth of K18 WT monitored by thioflavin fluorescence. Growth of 100% K18 WT onto K18 WT seeds (black traces) was compared with K18 WT growth in the presence of a) 2% spin labeled K18 311/328 (red trace) and b) 2% K18 311/328 ΔK280 (blue trace). Protein concentrations = 10 μM. Seed concentration = 4% (based on monomer concentration). Thioflavin T concentration = 5 μM. All values represent mean ± s.d. (n = 3 experiments). Spin labeled K18 311/328 and its ΔK280 variant do not affect the overall growth characteristics of K18 WT.

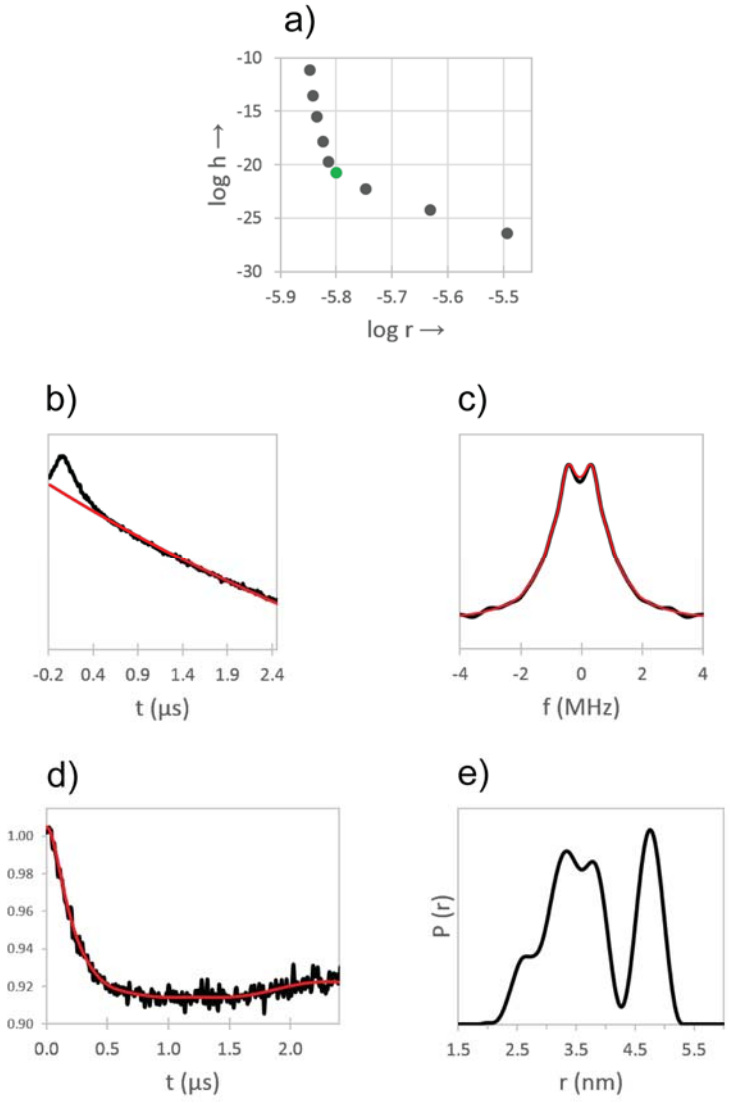

Figure S4. Distance distribution for K18 311/328 fibrils grown in the presence of K18 ΔK280. 10% K18 WT seeds were mixed with 50 µM tau monomers (96% K18 WT, 2% spin-labeled K18 311/328, and 2% K18 ΔK280) and 12.5 µM heparin. After overnight incubation at 37 °C, DEER data were collected from the sedimented fibrils. a) L-curve. b) Background fit. c) Pake pattern. d) Background subtracted DEER data. e) Distance distribution. Fit lines are in red, and α = 100 is in green on the L-curve. Based on the inherent heterogeneity of seeds, small variations in peak heights are expected for different seed batches. The similarity in distance distributions for fibrils formed in the presence e) and absence (Figure 1) of K18 ΔK280 suggests that the mutant does not alter the selection properties of spin labeled K18 311/328. Different mutants select different conformers based on their structural compatibility.

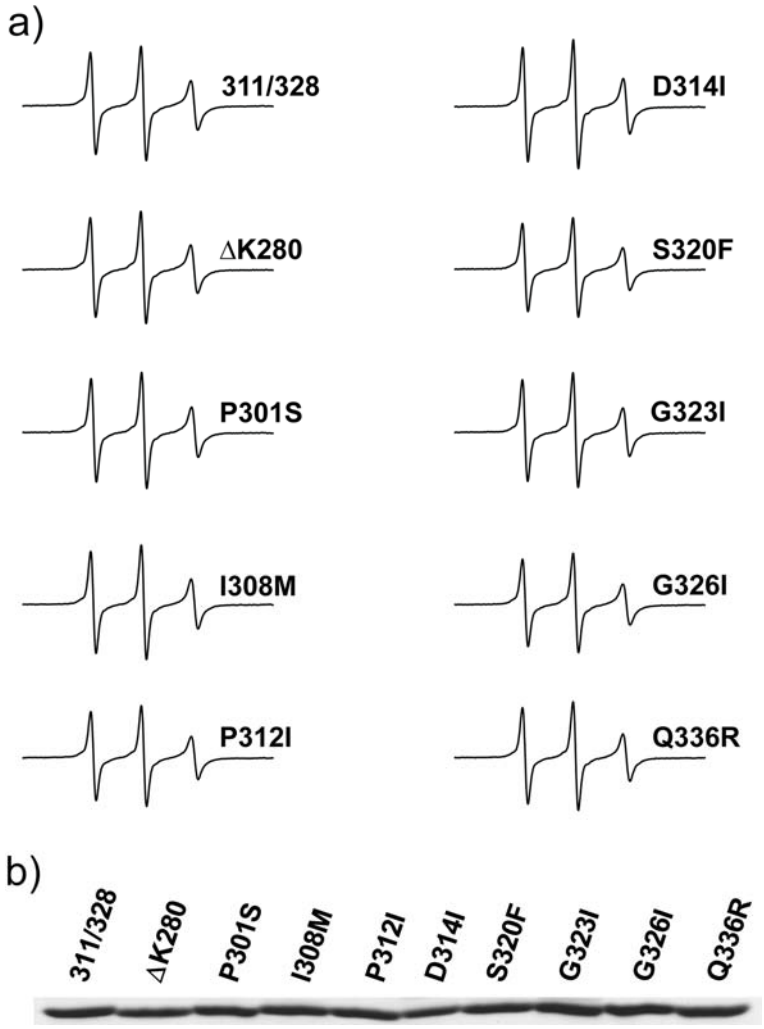

Figure S5. Labeling efficiencies of K18 monomers. a) CW EPR spectra of K18 311/328 and respective variants. b) Coomassie staining of spin-labeled K18 monomers after SDS PAGE. The gel verifies that equal protein concentrations were applied. The EPR data indicate that all mutants were labeled with similar efficiencies. Scan width = 150 G. The y axis, in arbitrary units, is the same for all mutants.

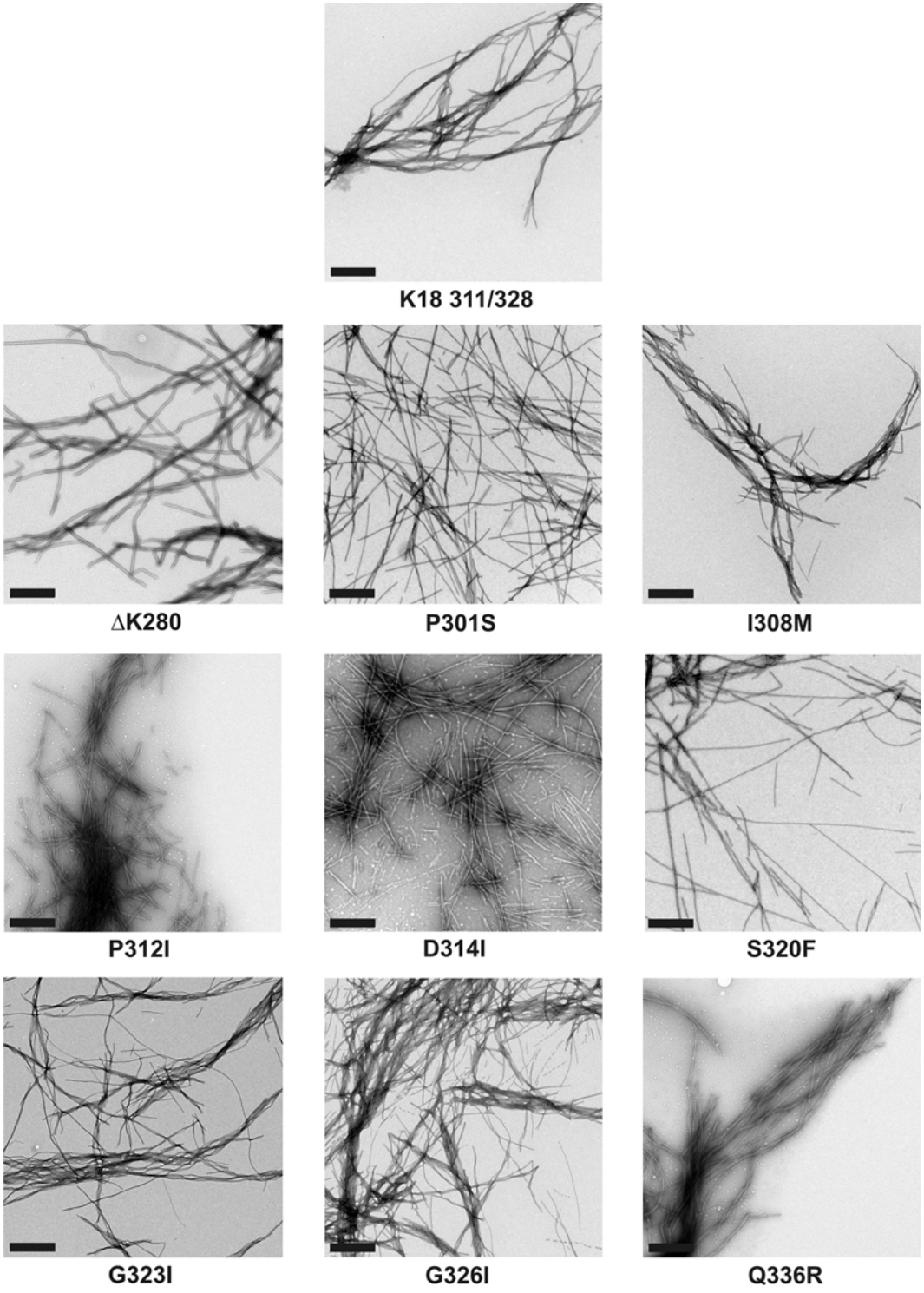

Figure S6. Electron micrographs of spin labeled K18 fibrils (labeled at positions 311 and 328) with (bottom rows) or without (top row) added mutations. Bar = 500 nm.

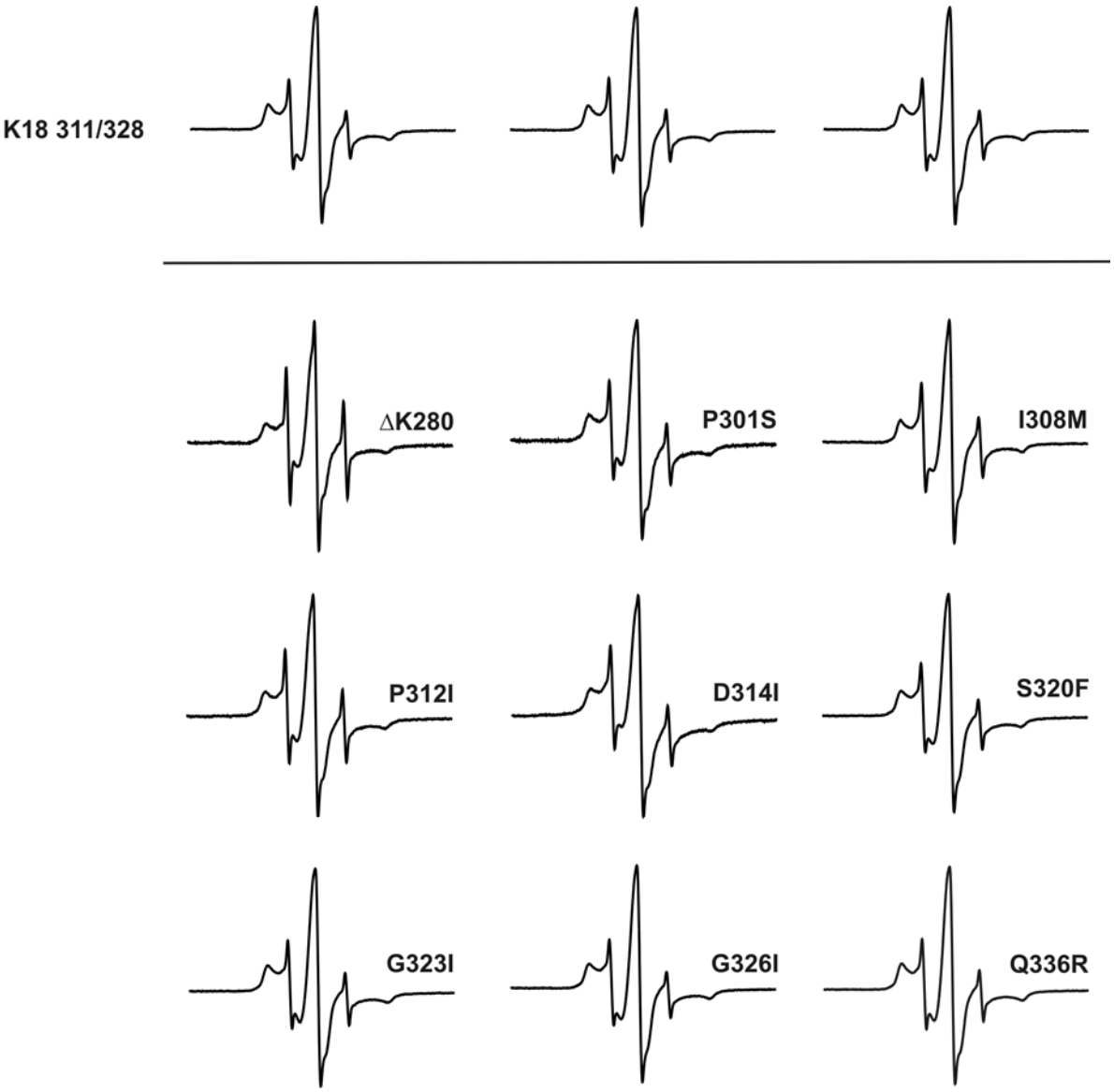

Figure S7. CW EPR spectra of spin labeled mutant K18 fibrils (1:50 molar ratio of spin labeled K18 mutant to K18 WT) at 298 K. Triplicate samples of non-mutated K18 311/328 are shown along the top row. Spectra reveal that spin labeled proteins are incorporated into the fibrils and that the labels are immobilized due to close packing within the fibrils. The absence of major spectral broadening indicates the absence of large subpopulations of conformers with short electron-electron distances. The sharp peaks, which account for less than 2% of the total spins, represent mobile spin labels (presumably from minor quantities of monomeric tau). Scan width = 150 G.

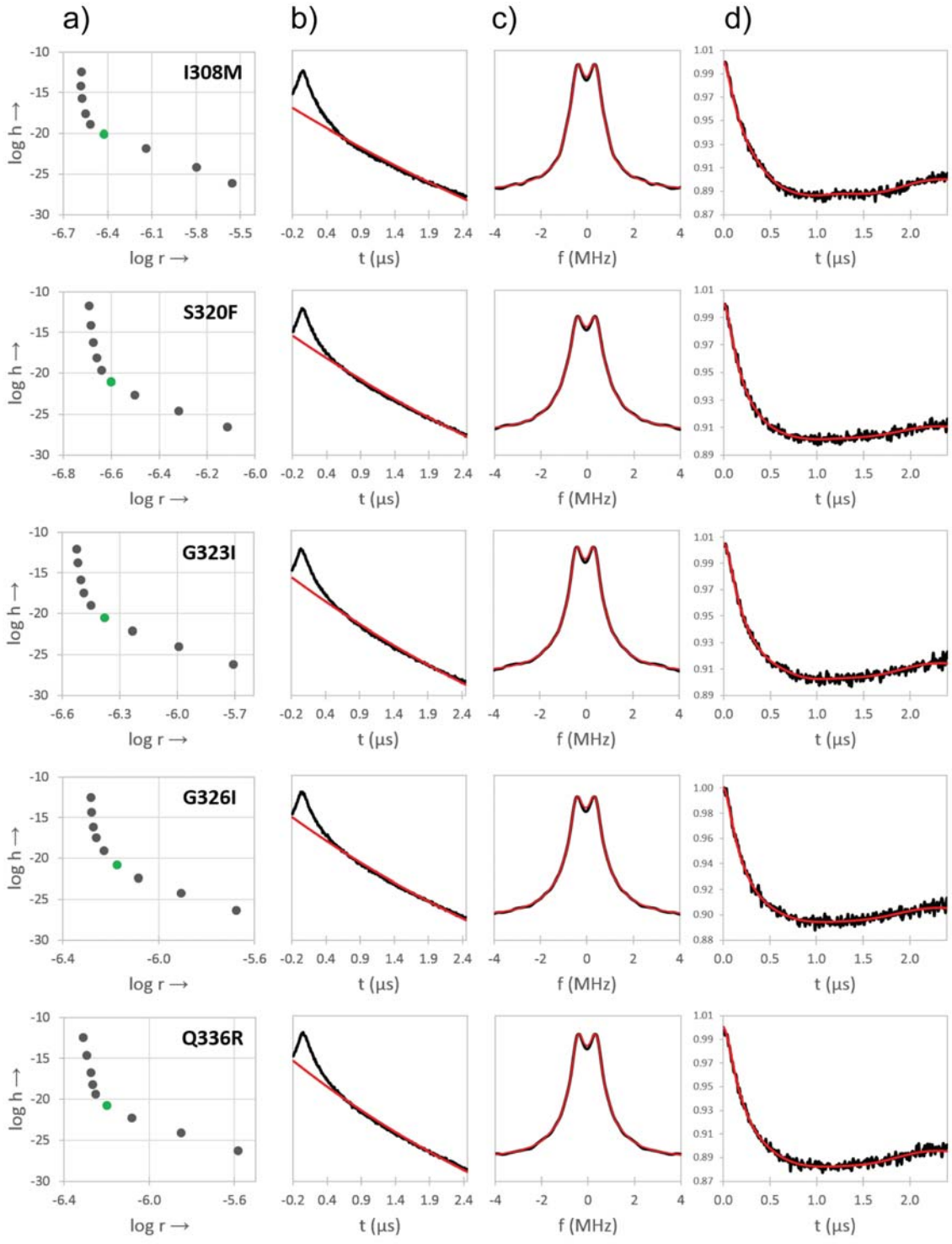

Figure S8. DEER data analysis of K18 mutants resulting in similar distance distributions. All proteins are spin-labeled at positions 311/328. a) L-curves. b) Background fits. c) Pake patterns. d) Background subtracted DEER data. Fit lines are in red, and α = 100 is in green on the L-curve. The different rows represent different tau mutants.

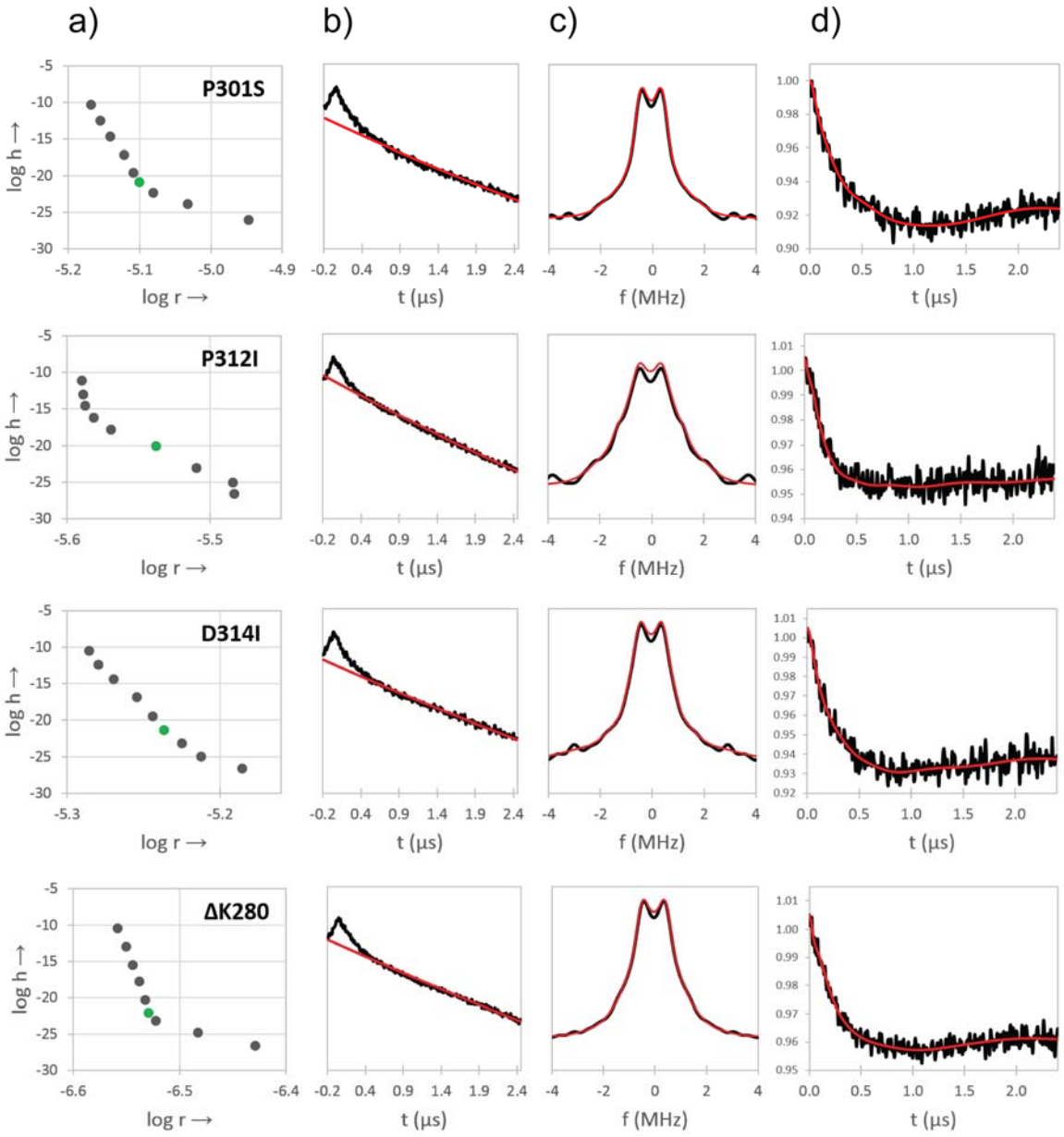

Figure S9. DEER data analysis of K18 mutants resulting in dissimilar distance distributions. All proteins are labeled at positions 311/328. a) L-curves. b) Background fits. c) Pake patterns. d) Background subtracted DEER data. Fit lines are in red, and α = 100 is in green on the L-curve. The different rows represent different tau mutants. The decreased signal-to-noise observed in d) compared to Figures S1 and S8 is attributed to a smaller number of spin pairs that are within the measurable range and increased populations of extended conformers with interspin distances that are too long to measure and therefore do not contribute to the signal. Importantly, a reduction in the number of scans for K18 311/328, which resulted in similar signal-to-noise levels as shown in d), had little effect on the overall peak positions (Figure S10), further corroborating that the mutations and not the signal-to-noise are the origin for the observed differences.

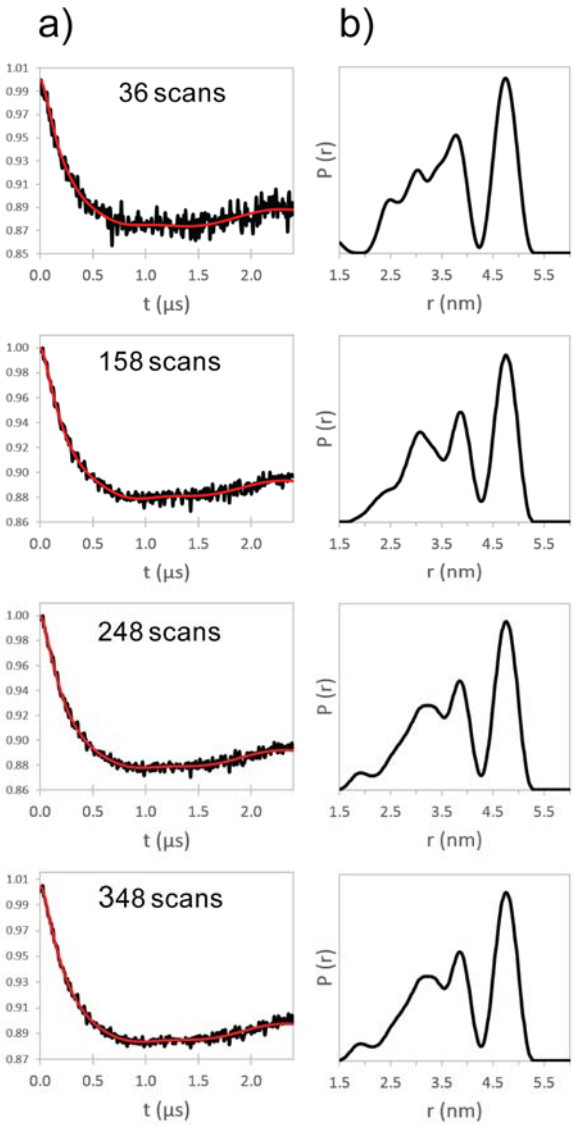

Figure S10. The effect of signal-to-noise on distance distributions in K18 311/328 fibrils. a) Background subtracted DEER data for different number of scans on the same sample. b) Corresponding distance distributions. The overall peak positions are unaffected by changes in signal-to-noise.

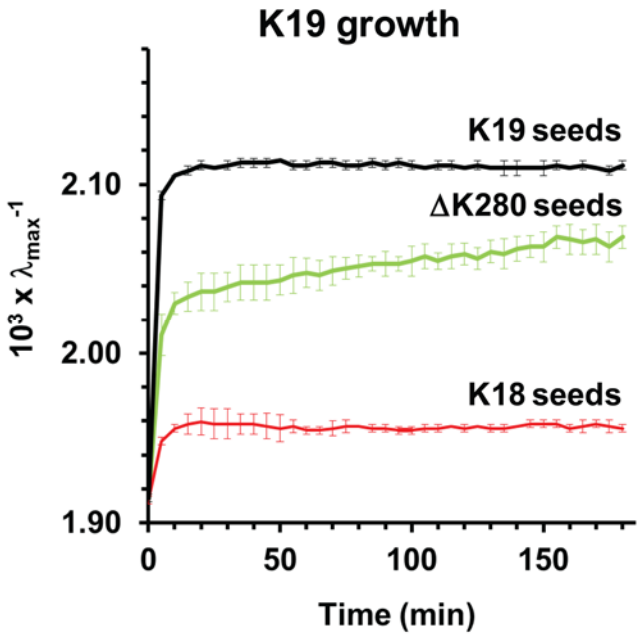

Figure S11. K19 growth characteristics depend on the identity of added seeds. K19 monomers (98% K19 WT plus 2% K19 labeled at position 310 with acrylodan) were mixed with 10% seeds. The inverse emission maxima are plotted as a function of time. Red trace = K18-seeded reaction; green trace = ΔK280-seeded reaction; black trace = K19-seeded reaction. Protein concentrations = 10 μM. All values represent mean ± s.d. (n = 3 experiments). Whereas growth onto K18 seeds is inhibited by a distinct barrier, growth onto ΔK280 seeds is not. Notice, that growth onto K19 seeds is most efficient. These data suggest different populations of conformers in the three types of seeds. K19 seeds result in maximal compatibility. Each fibril conformer is capable of recruiting K19 monomers. ΔK280 seeds show intermediate compatibility. A significant population of fibril conformers is capable of recruiting K19 monomers. K18 seeds show minimal compatibility. In these seeds only a minor sub-fraction of conformers is able to recruit K19 monomers. The lack of structural compatibility between K19 monomers and K18 seeds provides a molecular explanation for the observed seeding barrier.

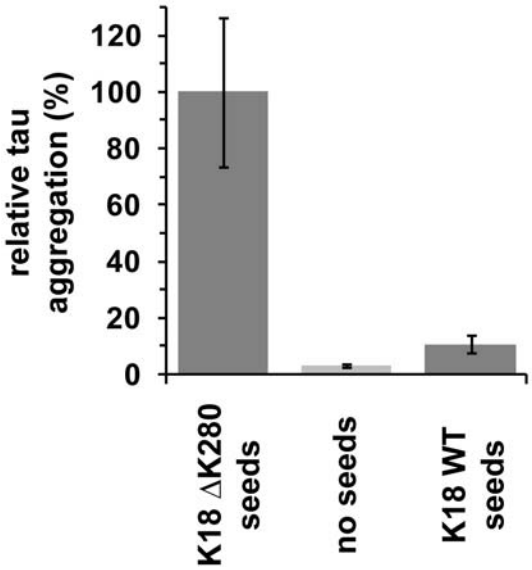

Figure S12. K19 WT (10μM) was grown on 10% seeds of ΔK280 K18 or K18 WT fibrils with 20 μM heparin. After 3 hours of incubation aggregates were sedimented, analyzed by SDS PAGE and quantified according to band density of aggregated K19 monomer. Values represent the mean ± SEM (n = 3).

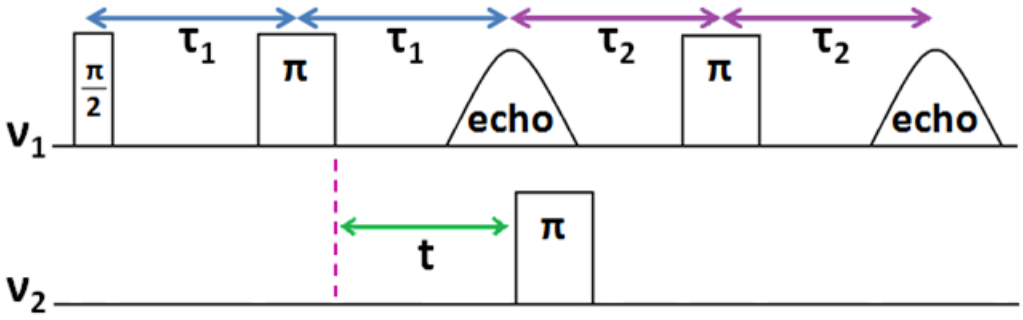

Figure S13. DEER pulse sequence. Following two pulses at ν_1, an echo is formed that refocuses after a third pulse is applied. This echo decays with time. A fourth pulse at a different frequency, ν_2, excites a separate part of the spectrum. If there are interactions between spins with resonance at ν_1 and ν_2, the amplitude of the detected echo depends on the time t. The distance between the spin labels can be extracted from the strength of their interaction, which determines the periodicity of the variation in echo intensity.

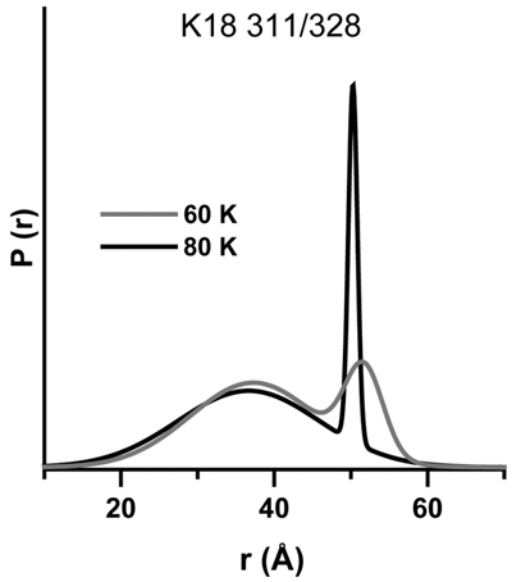

Figure S14. Comparison of distance distributions obtained using GLADD for fits to two Gaussian distributions of distances based on analysis of raw data obtained with time windows of 2.4 μs (80 K) and 3.4 μs (60 K). The sharp peak at 4.8 nm broadens as the length of the time window is increased, which provides better definition of the spin-spin interactions.

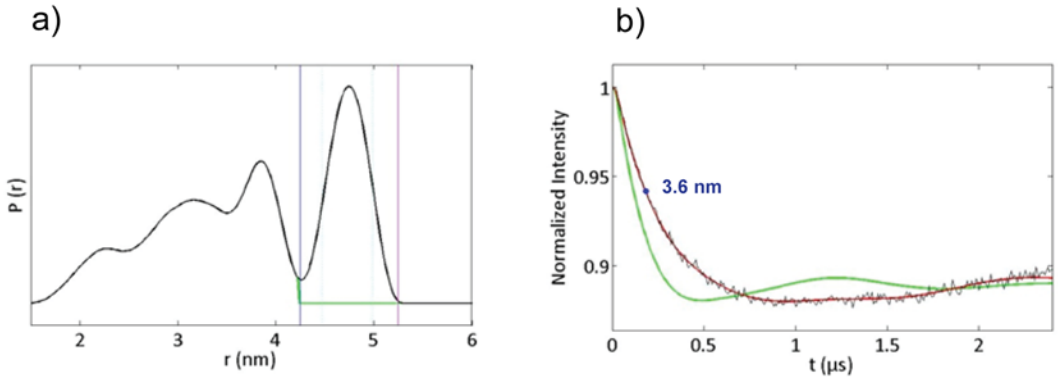

Figure S15. Peak suppression. When the peak suppression option of DEERAnalysis was used to exclude the main peak at 4.8 nm a), the agreement between the simulation (green trace, b) and the experimental background-subtracted DEER data (black trace, b) was much poorer than when the peak at 4.8 nm was included (red trace, b).

REFERENCES

[1] A. Siddiqua, Y. Luo, V. Meyer, M. A. Swanson, X. Yu, G. Wei, J. Zheng, G. R. Eaton, B. Ma, R. Nussinov, S. S. Eaton, M. Margittai, *J. Am. Chem. Soc.* **2012**, *134*, 10271-10278.

[2] A. Siddiqua, M. Margittai, *J. Biol. Chem.* **2010**, *285*, 37920-37926.

[3] H. Sato, V. Kathirvelu, A. J. Fielding, S. E. Bottle, J. P. Blinco, S. Micallef, S. S. Eaton, G. R. Eaton, *Mol. Phys.* **2007**, *105*, 2137-2151.

[4] H. Sato, V. Kathirvelu, G. Spagnol, S. Rajca, S. S. Eaton, G. R. Eaton, *J. Phys. Chem. B* **2008**, *112*, 2818-2828.

[5] G. Jeschke, V. Chechnik, P. Ionita, A. Godt, H. Zimmermann, J. Banham, C. R. Timmel, D. Hilger, H. Jung, *Appl. Magn. Reson.* **2006**, *30*, 473-498.

[6] S. Brandon, A. H. Beth, E. J. Hustedt, *J. Magn. Reson.* **2012**, *218*, 93-104.

[7] P. D. Dinkel, A. Siddiqua, H. Huynh, M. Shah, M. Margittai, *Biochemistry* **2011**, *50*, 4330-4336.